ARCHIVIO ISTITUZIONALE
DELLA RICERCA

Alma Mater Studiorum Università di Bologna
Archivio istituzionale della ricerca

Wake-Up Radio Impact in Self-Sustainability of Sensor and Actuator Wireless Nodes in Smart Home Applications

This is the final peer-reviewed author's accepted manuscript (postprint) of the following publication:

Published Version:
Wake-Up Radio Impact in Self-Sustainability of Sensor and Actuator Wireless Nodes in Smart Home Applications / Perilli L, Franchi Scarselli E, La Rosa R, Canegallo R. - ELETTRONICO. - Catalog Number: CFP1828K-ART:(2018), pp. 1-7. (Intervento presentato al convegno 2018 Ninth International Green and Sustainable Computing Conference (IGSC) tenutosi a Pittsburgh, Pennsylvania, USA nel 22 October – 24 October, 2018) [10.1109/IGCC.2018.8752164].

Availability:
This version is available at: https://hdl.handle.net/11585/664142 since: 2020-02-20

Published:

DOI: http://doi.org/10.1109/IGCC.2018.8752164

Terms of use:

Some rights reserved. The terms and conditions for the reuse of this version of the manuscript are specified in the publishing policy. For all terms of use and more information see the publisher's website.

This item was downloaded from IRIS Università di Bologna (https://cris.unibo.it/).
When citing, please refer to the published version.

(Article begins on next page)

23 April 2024

This is the post peer-review accepted manuscript of:
L. Perilli, E. Franchi Scarselli, R. La Rosa and R. Canegallo, "Wake-Up Radio Impact in Self-Sustainability of Sensor and Actuator Wireless Nodes in Smart Home Applications," *2018 Ninth International Green and Sustainable Computing Conference (IGSC)*, Pittsburgh, PA, USA, 2018, pp. 1-7.

The published version is available online at:
https://doi.org/10.1109/IGCC.2018.8752164

©2018 IEEE. Personal use of this material is permitted. Permission from IEEE must be obtained for all other uses, in any current or future media, including reprinting/republishing this material for advertising or promotional purposes, creating new collective works, for resale or redistribution to servers or lists, or reuse of any copyrighted component of this work in other works.

Wake-Up Radio Impact in Self-Sustainability of Sensor and Actuator Wireless Nodes in Smart Home Applications

L. Perilli, E. Franchi Scarselli
ARCES-DEI, University of Bologna
Bologna, Italy
luca.perilli@unibo.it, eleonora.franchi@unibo.it

R. La Rosa, R. Canegallo
STMicroelectronics
Catania, Agrate Brianza, Italy
roberto.larosa@st.com, roberto.canegallo@st.com

Abstract—This work discusses the impact of Wake-Up Radio (WuR) technology to extend the battery life on sensor and actuator nodes in a smart home scenario. The focus is on nodes that harvest energy from light or a temperature gradient and implement DASH7, an open-source low-power protocol supporting both *query-response* and *beaconing* communication models. A prototype WuR is used, with a quiescent current less than 1 µA and a sensitivity of -38 dBm compatible with indoor applications. Experimental data show that integrating WuR is not convenient in nodes that need to send a message to the network coordinator periodically, e.g. sensor nodes implementing *beaconing* communication models. On the contrary, in *request-response* mode, integrating the WuR, the average actuator current consumption reduces from 35 µA down to 6 µA during a reference period where no data or commands are exchanged between the network coordinator and the node. Thanks to the WuR, we find that an average light intensity of 150 lux throughout daytime and less than 14 min of a temperature gradient of 10°C between the hot and cold side of a thermoelectric generator are sufficient to turn the actuator nodes for water flooding and smart heating control into an energetically autonomous mode.

Keywords-energy harvesting; WSAN; Internet of Things; low-power protocol; Wake-Up Radio

I. INTRODUCTION

Wireless Sensor and Actuator Networks (WSAN) refer to a group of sensors and actuators linked by a wireless medium and providing services for the end user. They perform distributed sensing and automate interactions with the environment, and designers of WSAN must take into account trade-offs between several different performance indicators such as range, power consumption, latency [1], data throughput and application functionalities.

A big challenge in this area of research is the limited battery lifetime that affects the pervasiveness of the network, not only because of battery costs but also for the high maintenance costs. Various strategies and technologies are used to achieve energy efficiency and a consequent increase in battery life, such as using lightweight communication and MAC protocols [2], adopting low power radio transceivers [3], or using energy harvesting devices [4]. As the radio consumption is the largest contributor to a node power budget, Wake-Up Radio (WuR) technology has recently been proposed as a technique for turning off the main transceiver while communication is not needed, see for example [5][6][7] and [8] where an extensive survey of WuR research activity is presented.

Purpose of this paper is to discuss the effectiveness of WuR technology to extend the battery life of sensing and actuating nodes in a Wireless Sensor and Actuator Network for smart home application. To this aim, we designed a prototype network implementing two tasks representative of this application area: smart heating control and water flooding control. The first application controls radiator-based heat distribution through temperature sensor nodes and motor actuator nodes that drive a brushed DC motor connected to the radiator valve; the second application senses water flooding and controls a motor actuator node driving a brushed DC motor connected to the water supply system and able to cut off the water flow. Energy is harvested from light and from a temperature gradient. Connectivity between nodes and a network coordinator is provided by DASH7, a low-power open source communication protocol [10][11]. Sensor and actuator nodes have different constraints in terms of latency and data rate. To minimize the power consumption of the proposed WSAN, two types of communication methods are used and WuR is integrated in the actuator nodes.

The paper proceeds as follows: Section II presents the proposed WSAN system prototype and describes the node architecture and the energy harvesting sources. The two communication models made available by DASH7 protocol are discussed in Section III, considering the most suitable one for different types of nodes, while the integration of a Wake-Up Radio in actuator nodes is described in Section IV. Section V discusses the nodes' energy balance and presents the results in terms of system self-sustainability. Finally, in Section VI some conclusions are drawn.

II. DESCRIPTION OF THE PROPOSED WSAN

A. System Architecture

The proposed indoor WSAN (Fig. 1) consists of sensor

nodes, actuator nodes, a coordinator and an IoT gateway to connect the WSAN to Internet and the Cloud. The network architecture has a star structure, where all the nodes communicate with the coordinator. The WSAN implements two tasks: smart heating control and water flooding control. The first application is based on temperature sensor nodes supplied by an indoor photovoltaic (PV) harvester and actuator nodes, supplied by a thermoelectric generator (TEG) harvester connected to the radiator hot pipe, that drive a brushed DC motor connected to the radiator valve.

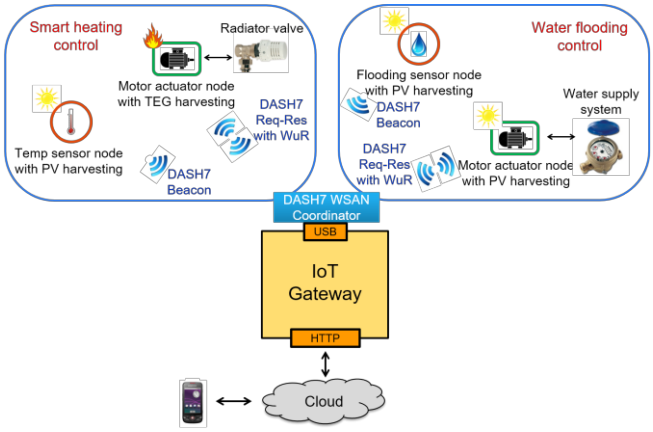

Figure 1. System architecture of the indoor autonomous WSAN.

The second consists of a water flood sensor node and an actuator node driving a brushed DC motor connected to the water supply system to cut off water flow, both supplied by indoor photovoltaic (PV) harvesters.

Connectivity between nodes and the network gateway is provided by DASH7 [10][11] protocol that supports two communication models: the pull model for a query-response method (e.g. smart heating control) and the push model for data transfer initiated from the nodes (e.g. sensor alarms). The coordinator of the DASH7 network is externally powered and connected to the Internet through an IoT gateway which makes the nodes visible to a remote server through HTTP messages [9].

B. Node Architecture

Sensor and actuator nodes share the same architecture: as shown in Fig. 2, they consist of a low-power microcontroller (STM32L1 [12]), a sub-GHz radio for data communication (SPIRIT1 [13]) and sensor devices and/or actuator devices. The nodes include a Power Unit composed of a power management system that interacts with indoor PV or TEG transducers for energy harvesting, and a rechargeable battery [9].

A real-time Operating System (OS) runs on an STM32L1 microcontroller (MCU) and manages the DASH7 protocol stack, the radio activity and the sensor and actuator operations. STM32L1 has various low-power states whose current consumption is up to about 1.5 µA.

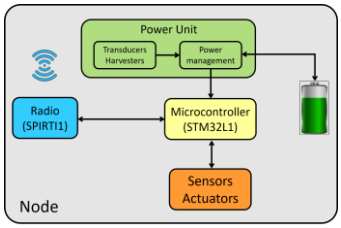

Figure 2. Sensor/actuator node architecture.

The SPIRIT1 low-power RF transceiver operates in the sub-GHz band and supports different modulation schemes; the operating frequency can be programmed in the range 169-915 MHz. In the proposed network the frequency adopted is 433 MHz. In the *sleep* state the current consumption is about 1 µA.

STTS751 [14] measures the ambient temperature at a user-configurable resolution between 9 and 12 bits with a sampling rate up to 32 conversions per second; its stand-by current consumption is around 3 µA. The flooding sensor is implemented through a custom circuit that measures impedance changes between two electrodes in order to detect the presence of water; its static current consumption is about 2 µA. In the actuator nodes, DRV8830 [15], a device especially designed for battery-powered and low-voltage motion control applications, drives a low-voltage brushed DC motor connected to the radiator valve or to the water supply system, respectively. The current consumption of the motor driver in the *sleep* state is about 1 µA.

The OS puts the microcontroller and the rest of the node in a *sleep* state when there are no operations to perform. As shown in Fig. 1, each node in the proposed WSAN includes only one sensor or one actuator. The current consumption of the whole node in the *sleep state* is roughly the same as for the different types of node and is about 5 µA.

C. Power Unit

In the Power Unit, the power management system draws off energy from the harvester sources and the rechargeable battery to supply the node, and, if harvested power exceeds demand, the remaining energy is used to recharge the battery. The power management system integrates an ultra-low power and high-efficiency energy harvester dc-dc converter and battery charger (SPV1050 [16]), which implements a Fractional Open-Circuit Voltage (FOCV) Maximum Power Point Tracking (MPPT) [17] function to optimize the power generated by the harvesting source and integrates the switching elements of a buck-boost converter.

Only energy sources mainly available in an indoor scenario and suitable for the proposed application are taken into account. These are light, both artificial and natural, and the temperature gradient. RF waves, despite being present in the environment (WiFi, GSM, etc.), are not considered as they provide less energy than the other sources and not enough for the requirement of our application [18], even though recent prototypes for dedicated applications have been presented [19].

We use indoor photovoltaic cells (two AM-1801 panels in series) connected to the SPV1050 dc-dc converter; this harvesting system provides, at the output of the converter, a current of 18 µA up to 220 µA with a light intensity varying from 115 lux to 1000 lux, as shown in Table I, which reports some experimental results. The last column of Table I also shows the charge supplied by the PV harvesting system (Q_{HARV_PV}) in a reference interval T_{REF} = 60 s, calculated using the following relation

$$Q[C] = I[A] * T[s]. \quad (1)$$

TABLE I. EXPERIMENTAL RESULTS OF CURRENTS AND CHARGES GENERATED FROM THE PV HARVESTING SYSTEM

Light intensity (lux)	I_{HARV_PV} (µA)	Q_{HARV_PV} (mC)
115	18	1.08
150	25	1.5
200	40	2.4
300	60	3.6
400	75	4.5
500	120	7.2
700	150	9
900	200	12
1000	220	13.2

Fig. 3 shows the Power Unit board equipped with the photovoltaic harvesting system. In Fig.4 an experimental measurement of harvested current over time is shown under changing indoor light intensity; values from 100 to 300 lux

Figure 3. Power Unit board equipped with the PV harvesting system.

are the average illuminance levels in a typical home scenario.

The Power Unit with its photovoltaic harvesting system, as shown in Fig. 3, is used for the temperature sensor node in the smart heating control application and for both the flooding sensor node and the motor actuator node in the water flooding control application.

The actuator node in the smart heating control application is connected, through a brushed DC motor, to a radiator valve to tune the flow of hot water; a TEG from Micropelt [20] connected to the hot pipe of the radiator is used as the harvesting system. Fig. 5 shows the hardware of the actuator node with the radiator valve and the harvesting board including the TEG; Fig. 6 shows the experimental measurement of the current generated from the harvester.

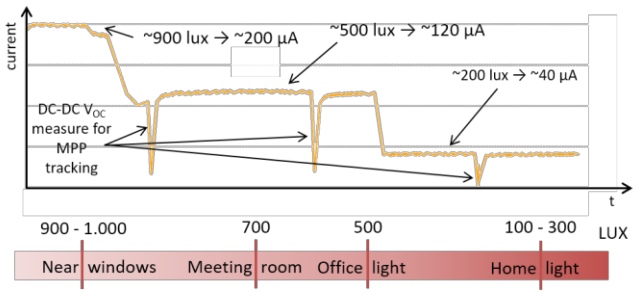

Figure 4. Experimental measurement of the photovoltaic harvested current over time under changing light intensity (top), and typical indoor light intensities (bottom).

The TEG is placed in contact with the hot pipe of the radiator and, with a temperature difference of about 8-10 °C between the hot and cold side of the TEG, a current I_{HARV_TEG} of about 220 µA is measured, which corresponds to a charge Q_{HARV_TEG} = 13.2 mC supplied to the load in a reference period T_{REF} = 60 s (1). Current acquisition was performed only at the specified temperature difference because the TEG placed in contact with the radiator hot pipe represents the real case in which the system has to work.

The negative peaks in the current waveforms of Fig. 4 and Fig. 6 correspond to periodic readings of the transducer open-circuit voltage (V_{OC}) implemented by the FOCV MPPT algorithm to track variations in operating conditions. During these phases the dc-dc converter does not supply current to the load.

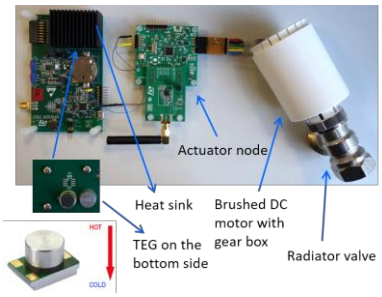

Figure 5. Actuator node connected to the radiator valve with TEG harvesting system.

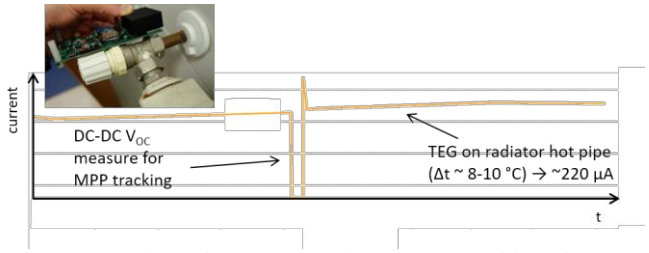

Figure 6. Experimental measurement of current generated from the TEG harvester placed in contact with the radiator hot pipe.

III. COMMUNICATION PROTOCOL: PUSH AND PULL MODELS

Wireless connectivity is what most heavily affects total power consumption and different low-power radio technologies and protocols (e.g. LoRaWAN, Sigfox, BLE, ZigBee) have been proposed to face this problem.

We use DASH7 communication protocol on STMicroelectronics SPIRIT1 sub-GHz radio. DASH7 [10][11] is an open source WSAN protocol which operates in the 433 MHz, 868 MHz and 915 MHz unlicensed ISM band. It can achieve a data rate of 200 kbps and an outdoor range up to 2 km and is based on the ISO/IEC 18000-7 standard for RFID devices. A key feature of this open source protocol is that it supports two communication models: a *pull* model for a query method (*request-response*) and a *push* model for data transfer initiated from the nodes (*beaconing*). The two modes can coexist in the same network and in the same node and allow us to use different communication methods in order to obtain optimum energy efficiency and response latency, depending on the node operation.

In *request-response* mode (or *pull* model) the communication between the nodes and the coordinator is bidirectional though the nodes can send data only after a coordinator request. This communication model thus allows the coordinator to acquire data from sensor nodes on request or to require execution of commands in actuator nodes (for example to drive a DC motor connected to a valve).

With reference to Fig. 7 [9], the DASH7 coordinator, before sending the *request* (Foreground or FG packet), transmits a sequence of short packets (Background or BG packets) to notify the listening nodes that a *request* will be sent with a specified delay; T_{FLOOD} is the duration of the BG packets sent by the coordinator, whose payload is the decreasing time left before the scheduled *request* packet. DASH7 nodes periodically scan the air (BG scan) at T_{SCAN} intervals looking for BG packets, alternating scans and sleep periods (*stand-by phase* in Fig. 7); the nodes need to capture one BG packet to know that the coordinator is about to send a *request* and begin a *data communication phase*. In order to ensure this synchronization, it is mandatory to program $T_{SCAN} < T_{FLOOD}$. In this way the coordinator and the nodes synchronize through an adjustable message scheduling technique and the nodes are able to capture each coordinator *request*.

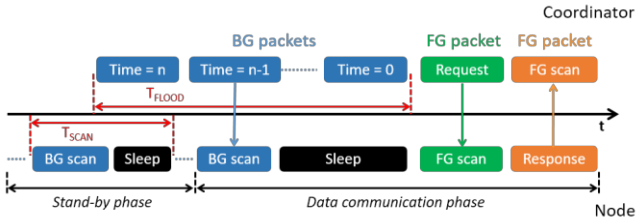

Figure 7. Scheme, not in scale, of the DASH7 *request-response* communication method.

One may program the T_{SCAN} and T_{FLOOD} intervals to obtain the best trade-off in terms of current consumption and responsiveness, since a high value of T_{SCAN} implies a reduction in the average *stand-by phase* current of the node and an increase in latency (equal to T_{FLOOD}), and vice versa. The best trade-off between the average current and the request latency is application-dependent and in the proposed application $T_{SCAN} = 4$ s and $T_{FLOOD} = 5$ s were chosen because the trade-off between a latency of 5 s between the request and motor actuation and the average *stand-by phase* current of the actuator nodes is reasonable both for a smart heating application and for water flooding control.

Fig. 8 shows the measured current in orange whereas red indicates the power supply of an actuator node using the *request-response* communication mode. The measured current includes the contribution of all the devices in Fig. 2, with the motor off.

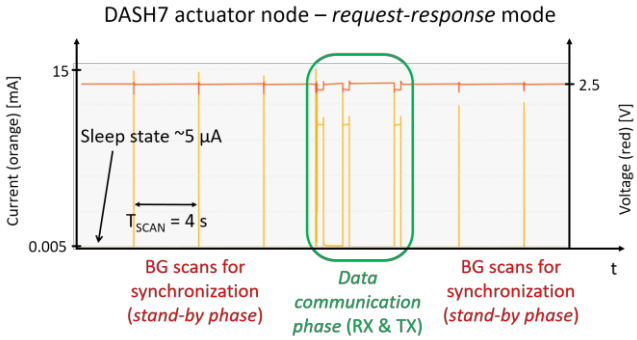

Figure 8. Experimental measurement of the current consumption of the DASH7 actuator node in *request-response* mode.

It can be seen how the node periodically wakes-up from the *sleep state* to perform receiving scan phases (BG scan) needed for node-coordinator synchronization (*stand-by phase*), according to Fig. 7. In the *sleep state* the current consumption of the node is about 5 µA, as reported in Section II-B. The current peaks corresponding to BG scans are about 15 mA. In the measured setup, the scan interval T_{SCAN} is 4 s. In the green circle a *data communication phase* is shown, consisting of a synchronization packet reception (BG packet), a data packet reception (FG packet - *request*) and the *response* transmission. The node average current consumption, in a period $T_{REF} = 60$ s with only one *data communication phase*, is 200 µA whereas the average current consumption without data communication (only *stand-by phases*) is 35 µA (Table II).

In *beaconing mode* (or *push* model) the node periodically initiates communication sending a message to the coordinator at a programmable frequency, while for the rest of the time it remains in a *sleep state*. This involves lower average current consumption than the *request-response* method, but the communication is unidirectional (from node to coordinator) which is not suitable for applications that need data or commands sent on request, as is the case with actuator nodes driving the brushed DC motor connected to

the water supply system to cut off the water flow. By contrast, this beaconing communication model is necessary for sending alarm (e.g. flooding sensor nodes), or periodic "alive" messages.

Fig. 9 shows the measured current, in orange, of a node which uses the *beaconing* communication mode. It can be seen how the node periodically wakes-up from a *sleep state*

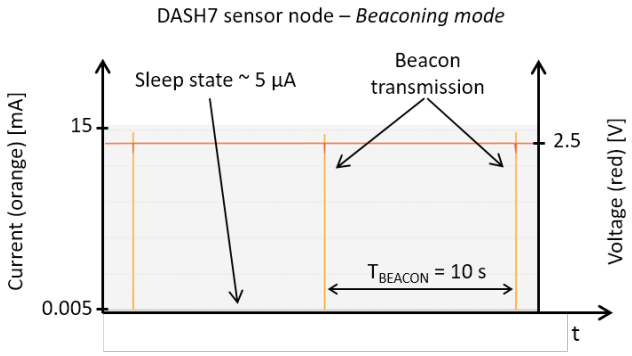

Figure 9. Experimental measurement of the current consumption of a DASH7 sensor node in *beaconing* mode; the current peaks here are message transmissions every 10 s.

to transmit sensor data. In the measured setup the interval between T_{BEACON} transmissions is 10 s and the node average current consumption, in T_{REF} = 60 s, is 14 µA (Table II).

TABLE II. COMPARISON OF THE NODE AVERAGE CURRENT CONSUMPTION AT AN INTERVAL T_{REF} = 60 S DEPENDING ON THE COMMUNICATION MODE WITH AND WITHOUT WAKE-UP RADIO

	Node Average Current Consumption		
	request-response (T_{SCAN} = 4 s)	*request-response with WuR*	*Beaconing* (T_{BEACON} = 10 s)
Stand-by phases with only one data communication phase in T_{REF}	200 µA	160 µA	14 µA
Only stand-by phases in T_{REF}	35 µA	6 µA	

IV. WAKE-UP RADIO IN ACTUATOR NODES

Wake-Up Radio (WuR) technology overcomes the trade-off between power consumption and responsiveness of *request-response* protocol by adding an ultra-low power radio receiver to the IoT node (Fig. 10), which monitors the communication channel while the node either stays in *sleep* mode or is disconnected from the power supply. Thus we get rid of the main radio activity required to maintain network synchronization (BG scans described in Section III), since a wake-up call sent by the coordinator before each data communication is detected by the always-on WuR that in turn activates the entire node: the normal *request-response* mechanism occurs and at the end the node returns to *sleep state*.

A Wake-Up Radio [21][22] developed by STMicroelectronics was used. Configured in *active* mode, the device has a current consumption of about 1 µA with a response time lower than 0.5 s and a radio sensitivity of -38 dBm, which, in free-space, allows one to turn on a WuR node from a distance ranging between 30 m and 50 m, with a transmitted power of 27 dBm, compatible with indoor applications.

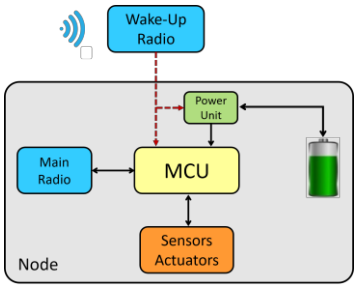

Figure 10. Node scheme with WuR.

By interfacing the WuR to the node, it is possible to keep the node in the *sleep state*, removing the periodic scan phases (BG scans), as shown in Fig. 11. When a wake-up call is detected the *data communication phase* occurs following the same behavior as shown in Fig. 8. Considering the WuR measured current consumption of about 1 µA, the total average consumption of the node, in a period of 60 s, decreases from 200 µA to 160 µA when there is one *data communication phase* whereas, with only *stand-by phases*, it decreases from 35 µA to 6 µA (Table II). Network synchronization is maintained thanks to the always-on WuR that monitors the communication channel continuously.

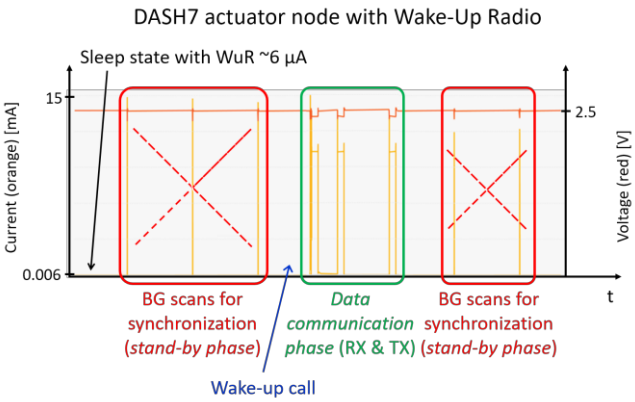

Figure 11. DASH7 actuator node behavior with WuR.

The introduction of WuR technology in the WSAN described thus leads to a reduction by about 80 % in the power consumption of the actuator node, considerably increasing the battery life.

V. Energy Balance for Sensor and Actuator Nodes

For a node to be autonomous or self-sustainable, the average harvested energy $E_{av,HARV}$ must be greater than the average energy consumed by the node $E_{av,SYS}$:

$$E_{av,HARV} \geq E_{av,SYS} \quad (2)$$

The battery only acts as an energy buffer: all the charge supplied to the node by the battery for an operation needs to be harvested and supplied to the rechargeable battery. Considering as the integration interval an integer n of the reference period T_{REF} = 60 s, since the power management system in the Power Unit (Fig. 2) keeps the supply voltage constant, (2) can be expressed in terms of charge balance

$$Q_{av,HARV} \geq Q_{av,SYS} \quad (3)$$

where typical values of $Q_{av,HARV}$ provided by the harvesters in indoor environment are those given in Section II-C while $Q_{av,SYS}$ depends on the node functionality.

A. Sensor Nodes with PV Harvesting

Both the temperature sensor node for smart heating control application and the flooding sensor node for water flooding control application use the *beaconing mode* of the DASH7 protocol and have roughly the same current consumption of 14 µA with a T_{BEACON} = 10 s, as reported in Table II. According to (1), the average charge consumption at a T_{REF} = 60 s of the sensor nodes is $Q_{av,SYS}$ = 0.84 mC. Comparing that value with the average charge provided by the PV transducer in Table I, it can be observed that (3) is satisfied when the light intensity is larger than or equal to 115 lux, corresponding to home light (Fig. 4). Moreover, an excess charge is available to keep the rechargeable battery at maximum level.

To evaluate the self-sustainability of the nodes, let us assume a dark period of 8 h, during which $Q_{av,HARV}$ = 0 and the charge absorbed by the node, from (1), is $Q_{av,SYS,DARK}$ = 403.2 mC. The time required to fully recharge the battery by the PV harvester with the excess charge during normal operation depends on the environment light intensity:

$$Q_{av,SYS,DARK} = n * (Q_{av,HARV} - Q_{av,SYS}) \quad (4)$$

where n is the integer number of reference periods T_{REF} = 60 s. The recharge time varies from about 10 h (n = 610) when the light intensity is 150 lux, 2.5 h (n = 146) with 300 lux down to about half an hour (n = 32.6) with 1000 lux.

B. Actuator Node with PV Harvesting for Water Flooding Control

In the water flooding control application, as described in Section II-B, the brushed DC motor must close the valve connected to the water supply system whenever a water flooding alarm is sent by the flooding sensor nodes. The actuator node therefore always operates in *stand-by phase* except during a *data communication phase* when the command to close the valve is sent by the coordinator. As previously discussed, the node uses a *request-response* communication model with a T_{SCAN} of some seconds gauged to provide good responsiveness for this specific application, at the cost of power consumption in *stand-by phase*. The trade-off between power and responsiveness is overcome by the use of the Wake-Up Radio, as is clear if one compares the experimental data in Table II.

The self-sustainability analysis of this node is similar to that described for sensor nodes with PV harvesting in the previous section, considering that the average node current consumption in *stand-by phase* is 6 µA instead of 14 µA which corresponds to $Q_{av,SYS}$ = 0.36 mC; what is more, (3) is satisfied for any light intensity starting from 115 lux. Considering the dark period of 8 h, self-sustainability of the node is evaluated using (4) at $Q_{av,SYS,DARK}$ = 172.8 mC; the resulting recharge time during the day varies from about 2.5 hours (n = 151) when light intensity is 150 lux, less than one hour (n = 53) with 300 lux down to less than 14 min with 1000 lux.

From the data on current consumption in Table II, it is important to note that, without WuR, $Q_{av,SYS}$ = 2.16 mC and (3) would only be satisfied for light intensity greater than 150 lux. In addition, the time to recharge the battery after an 8 h dark period would increase from less than one hour to more than 11 h with the excess charge provided by the PV harvesting at a light of 300 lux.

C. Actuator Node with TEG Harvesting for Smart Heating Control

The actuator nodes control a brushed DC motor and the power to drive the motor has to be provided by the node; therefore, the average charge absorbed by the node must take into account not only the current consumption due to communication with the coordinator, but also the current consumption supplied to the motor ($Q_{av,SYS,MOT}$). In the previous section discussing the water flooding control application, this term was not considered since a single motor action is required to react to an occasional alarm. In the smart heating control application, the current contribution of the motor cannot be ignored because the motor has to be moved frequently to track the desired temperature.

The limit of self-sustainability for the actuator node with TEG harvesting for the smart heating control application is imposed by the following relation:

$$n * Q_{HARV\_TEG} = (n - 1)\, Q_{av,SB} + (Q_{av,COMM} + Q_{av,SYS,MOT}) \quad (5)$$

where n is the integer number of reference interval T_{REF} between two actuating *requests*, Q_{HARV_TEG} = 13.2 mC is the charge generated by the TEG harvester, presumed constant as discussed in Section II-C, $Q_{av,SB}$ = 0.36 mC and $Q_{av,COMM}$ = 9.6 mC are respectively the charge consumption of the

node with WuR in *stand-by phase* and in *data communication phase* as calculated following (1) from current values in Table II, while $Q_{av,SYS,MOT}$ = 48 mC is the charge consumed by the motor to perform a movement equal to 10 % of the full valve range. Calculating n from (5), the actuator node is self-sustainable if motor actuation is performed at most every 5 min.

To evaluate the self-sustainability of the nodes let us assume a period of 8 h in a day where $Q_{HARV\_TEG} = 0$ since the water boiler is off and there is no temperature difference between environment and the water in the heating system. The charge absorbed by the node, from (1), is:

$$Q_{av,SYS,TOT} = Q_{av,SB} * 60 * 8 = 172.8\ mC. \quad (6)$$

The time to fully recharge the battery required by the TEG harvester using the excess charge during normal operation, assuming a temperature difference of 8–10 °C, is:

$$Q_{av,SYS,TOT} = n * (Q_{HARV\_TEG} - Q_{av,SB}) \quad (7)$$

where n, as before, is the integer number of reference intervals T_{REF} = 60 s. The recharge time is 13.5 min, whereas without WuR more than one and half hours is needed (n = 90).

VI. Conclusions

The paper discusses the impact of WuR technology to extend the battery life on sensor and actuator nodes in a prototype Wireless Sensor and Actuator Network (WSAN) for smart home application. Experimental data show that integrating WuR is not expedient when sensor nodes implement the *beaconing* communication model since the node functionality requires periodic messages to be sent to the coordinator (e.g. in water flooding sensor nodes). On the contrary, WuR technology overcomes the trade-off between power consumption and responsiveness of nodes implementing a *request-response* protocol by adding an ultra-low power radio receiver to the IoT node. Experimental results show that on integration with the WuR, the average actuator current consumption reduces from 35 µA down to 6 µA during a reference period where no data or commands are exchanged between the network coordinator and the node. Thanks to the WuR, we find that an average light intensity of 150 lux throughout the daytime after eight hours of darkness, and less than 14 min of a temperature gradient of 10°C between the hot and cold sides of a thermoelectric generator, are sufficient after eight hours with no energy harvested by the TEG to turn the actuator nodes for water flooding and smart heating control into an energetically autonomous mode.

Acknowledgment

This project received funding from the European Union's Horizon 2020 research and innovation programme under grant agreement No 730957.

References

[1] F. A. Aoudia, M. Magno, M. Gautier, O. Berder and L. Benini, "A Low Latency and Energy Efficient Communication Architecture for Heterogeneous Long-Short Range Communication," 2016 Euromicro Conference on Digital System Design (DSD), pp. 200-206.

[2] J. Oller, I. Demirkol, J. Casademont, J. Paradells, G. U. Gamm and L. Reindl, "Has Time Come to Switch From Duty-Cycled MAC Protocols to Wake-Up Radio for Wireless Sensor Networks?," in IEEE/ACM Trans. Netw., vol. 24, no. 2, pp. 674-687, April 2016.

[3] Z. Sheng, C. Zhu, V. C. M. Leung, "Surfing the Internet-of-Things: Lightweight Access and Control of Wireless Sensor Networks Using Industrial Low Power Protocols," EAI Endorsed Trans. Industrial Networks and Intelligent Systems, vol. 14, no. 1, 2014.

[4] P. Kamalinejad, C. Mahapatra, Z. Sheng, S. Mirabbasi, V. C. M. Leung, Y. L. Guan, "Wireless energy harvesting for the Internet of Things," IEEE Commun. Mag., vol. 53, no. 6, pp. 102-108, June 2015.

[5] I. Demirkol, C. Ersoy and E. Onur, "Wake-up receivers for wireless sensor networks: benefits and challenges," in IEEE Wireless Communications, vol. 16, no. 4, pp. 88-96, Aug. 2009.

[6] M. Magno, V. Jelicic, B. Srbinovski, V. Bilas, E. Popovici and L. Benini, "Design, Implementation, and Performance Evaluation of a Flexible Low-Latency Nanowatt Wake-Up Radio Receiver," in IEEE Trans. Ind. Informat., vol. 12, no. 2, pp. 633-644, April 2016.

[7] J.Estrada-Lopez, A.Abuellil, A. Costilla-Reyes, E. Sanchez-Sinencio, "Technology Enabling Circuits and Systems for the Internet-of-Things: An Overview",2018 Symp. on Circuits and Systems (ISCAS)

[8] R.Piyare, A.L.Murphy, C. Kiraly, P.Tosato, D. Brunelli, "Ultra Low Power Wake-up Radios: A Hardware and Networking Summary", IEEE Communications Surveys & Tutorials, vol. 19, no. 4, 2017.

[9] A. D'Elia, L. Perilli, F. Viola, L. Roffia, F. Antoniazzi, R. Canegallo, T. Salmon Cinotti, "A self-powered WSAN for energy efficient heat distribution," 2016 IEEE Sensors Applications Symposium (SAS).

[10] M. Weyn, G. Ergeerts, L. Wante, C. Vercauteren, P. Hellinckx "Survey of the DASH7 Alliance Protocol for 433 MHz Wireless Sensor Communication" International Journal of Distributed Sensor Networks, 2013, Volume 9, Issue 12.

[11] *DASH7 Alliance Protocol Specification v1.1*, http://www.dash7-alliance.org/product/d7ap1-1/.

[12] [Online] http://www.st.com/resource/en/datasheet/stm32l151c6.pdf.

[13] [Online] http://www.st.com/resource/en/datasheet/spirit1.pdf.

[14] [Online] https://www.st.com/resource/en/datasheet/stts751.pdf.

[15] [Online] http://www.ti.com/lit/ds/symlink/drv8830.pdf.

[16] [Online] www.st.com/resource/en/datasheet/spv1050.pdf.

[17] P.R.J.Kumar, "Design and overview of maximum power point tracking techniques in wind and solar photovoltaic systems: A review" Renewable and Sustainable Energy Reviews, June 20, pp. 73:1138-1159.

[18] James M. Gilbert, F. Balouchi, "Comparison of energy harvesting systems for wireless sensor networks" International Journal of Automation and Computing, Oct. 2008, Vol. 5, Issue 4, pp 334–347.

[19] M. Pizzotti, L. Perilli, M. del Prete, D. Fabbri, R. Canegallo, M. Dini, D. Masotti, A. Costanzo, E. Franchi Scarselli, A. Romani, "A Long-Distance RF-Powered Sensor Node with Adaptive Power Management for IoT Applications", Sensors, vol. 17, issue 8, 2017.

[20] [Online] http://www.micropelt.com/en/energy-harvesting/tgp.html.

[21] R. La Rosa, N. Aiello and G. Zoppi, "RF remotely-powered integrated system to nullify standby power consumption in electrical appliances," IECON 2016 - 42nd Annual Conference of the IEEE Industrial Electronics Society, Florence, 2016, pp. 1162-1164.

[22] R. Guerra, A. Finocchiaro, G. Papotto, B. Messina, L. Grasso, R. La Rosa, G. Zoppi, G. Notarangelo, G. Parmisano, "An RF-powered FSK/ASK receiver for remotely controlled systems," 2016 IEEE Radio Frequency Integrated Circuits Symposium (RFIC), pp. 226-229